r.sim.terrain 1.0: a landscape evolution model with dynamic hydrology

Brendan Alexander Harmon[1], Helena Mitasova[2,3], Anna Petrasova[2,3], and Vaclav Petras[2,3]

[1]Robert Reich School of Landscape Architecture, Louisiana State University, Baton Rouge, Louisiana, USA
[2]Center for Geospatial Analytics, North Carolina State University, Raleigh, North Carolina, USA
[3]Department of Marine, Earth, and Atmospheric Sciences, North Carolina State University, Raleigh, North Carolina, USA

Correspondence: Brendan Harmon (baharmon@lsu.edu)

Abstract. While there are numerical landscape evolution models that simulate how steady state flows of water and sediment reshape topography over long periods of time, r.sim.terrain is the first to simulate short-term topographic change for both steady state and dynamic flow regimes across a range of spatial scales. This free and open source, GIS-based topographic evolution model uses empirical models for soil erosion at watershed to regional scales and a physics-based model for shallow overland water flow and soil erosion at subwatershed scales to compute short-term topographic change. This model uses either a steady state or dynamic representation of overland flow to simulate how overland sediment mass flows reshape topography for a range of hydrologic soil erosion regimes based on topographic, land cover, soil, and rainfall parameters. As demonstrated by a case study for Patterson Branch subwatershed on the Fort Bragg military installation in North Carolina, r.sim.terrain can realistically simulate the development of fine-scale morphological features including ephemeral gullies, rills, and hillslopes. Applications include land management, erosion control, landscape planning, and landscape restoration.

1 Introduction

Landscape evolution models represent how the surface of the earth changes over time in response to physical processes. Most studies of landscape evolution have been descriptive, but a number of numerical landscape evolution models have been developed that simulate elevational change over time (Temme et al., 2013). Numerical landscape evolution models such as the Channel-Hillslope Integrated Landscape Development (CHILD) model (Tucker et al., 2001) and SIBERIA (Willgoose, 2005) simulate steady state flows over long temporal scales. Landlab, a new Python library for numerically modeling Earth surface processes (Hobley et al., 2017), has components for simulating landscape evolution such as the Stream Power with Alluvium Conservation and Entrainment (SPACE) model (Shobe et al., 2017). While Geographic Information Systems (GIS) support efficient data management, spatial and statistical modeling and analysis, and visualization, there are few GIS-based soil erosion models or landscape evolution models (see Tables **??**-**??**). Thaxton (2004) developed a GRASS GIS shell script module

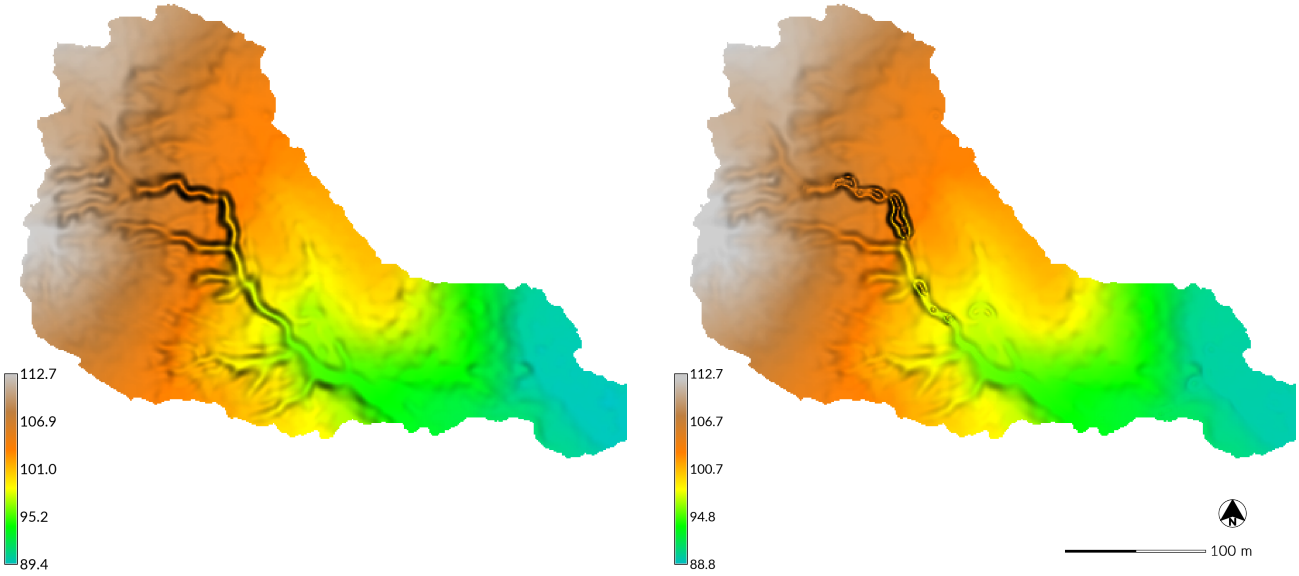

Figure 1. The digital elevation model (DEM) before (a) and after (b) simulated landscape evolution with r.sim.terrain for a subwatershed of Patterson Branch, Fort Bragg, NC, USA. This simulation used the SIMWE model for a 120 min rainfall event with 25 $\mathrm{mm\,hr^{-1}}$ in a transport limited soil erosion regime at steady state. In the evolved DEM (b) the gully channel has widened with depositional ridges forming along its thalweg.

r.terradyn to simulate terrain evolution by combining steady-state net erosion deposition rates estimated by the Simulation of Water Erosion (SIMWE) model (Mitas and Mitasova, 1998) and gravitational diffusion. Barton et al. (2010) implemented a long term landscape evolution GRASS GIS model r.landscape.evol which integrates gravitational diffusion, USPED model and fluvial erosion and has been applied to simulate impact of prehistoric settlements on mediteranean landscapes. However, there are still major research questions to address in the theoretical foundations of erosion modeling such as how erosional processes scale over time and space and how sediment detachment and transport interact (Mitasova et al., 2013). While most numerical landscape evolution models simulate peak flows at steady state (see Table **??**), short-term erosional processes like gully formation can be dynamic with significant morphological changes happening within minutes before flows reach steady state. A landscape evolution model with dynamic water and sediment flow is needed to study fine-scale spatial and short-term temporal erosional processes such as gully formation and the development of microtopography.

At the beginning of a rainfall event the overland water flow is unsteady – its depth changes at a variable rate over time and space. If the intensity of rainfall continues to change throughout the event then the flow regime will remain dynamic. If,

however, the overland flow reaches a peak rate then the hydrologic regime is considered to be at steady state. At steady state:

$$\frac{\partial h(x,y,t)}{\partial t} = 0 \tag{1}$$

where:

(x,y) is the position [m]

t is the time [s]

$h(x,y,t)$ is the depth of overland flow [m]

Gullies are eroded, steep banked channels formed by ephemeral, concentrated flows of water. A gully forms when overland waterflow converges in a knickzone – a concave space with steeper slopes than its surroundings (Zahra et al., 2017) – during intense rainfall events. When the force of the water flow concentrated in the knickzone is enough to detach and transport large amounts of sediment, an incision begins to form at the apex of the knickzone – the knickpoint or headwall. As erosion continues the knickpoint begins to migrate upslope and the nascent gully channel widens, forming steep channel banks. Multiple incisions initiated by different knickpoints may merge into a gully channel and multiple channels may merge into a branching gully system (Mitasova et al., 2013). This erosive process is dynamic; the morphological changes drive further changes in a positive feedback loop. When the gully initially forms the soil erosion regime should be detachment capacity limited with the concentrated flow of water in the channel of the gully detaching large amounts of sediment and transporting it to the foot of the gully, potentially forming a depositional fan. If the intensity of rainfall decreases and transport and detachment capacity approach a balance, then the soil erosion regime may switch to a variable erosion-deposition regime, in which soil is eroded and deposited in a spatially variable pattern. Subsequent rainfall events may trigger further knickpoint formation and upslope migration, channel incision and widening, and depositional fan and ridge formation. Between high intensity rainfall events, lower intensity events and gravitational diffusion may gradually smooth the shape of the gully. Eventually, if detachment capacity significantly exceeds transport capacity and the regime switches to transport capacity limited, the gully may fill with sediment, as soil continues to be eroded, but is not transported far.

Gully erosion rates and evolution can be monitored in the field or modeled on the computer. Field methods include dendrogeomorphology (Malik, 2008) and permanent monitoring stakes for recording erosion rates, extensometers for recording mass wasting events, weirs for recording water and suspended sediment discharge rates, and time series of surveys using total station theodolites (Thomas et al., 2004), unmanned aerial systems (UAS), airborne lidar, and terrestrial lidar (Starek et al., 2011; Bechet et al., 2016). With terrestrial lidar, airborne lidar and UAS photogrammetry there is now sufficient resolution topographic data to morphometrically analyze and numerically model fine-scale landscape evolution in GIS including processes such as gully formation and the development of microtopography. Gully erosion has been simulated with RUSLE2-Raster (RUSLER) in conjunction with the Ephemeral Gully Erosion Estimator (EphGEE) (Dabney et al., 2014), while gully evolution has been simulated for detachment capacity limited erosion regimes with the Simulation of Water Erosion (SIMWE) model (Koco, 2011; Mitasova et al., 2013). Now numerical landscape evolution models that can simulate steady state and unsteady

flow regimes and can dynamically switch between soil erosion regimes are needed to study fine-scale spatial and short-term temporal erosional processes.

The numerical landscape evolution model r.sim.terrain was developed to simulate the spatiotemporal evolution of landforms caused by shallow overland water and sediment flows at spatial scales ranging from square meters to kilometers and temporal scales ranging from minutes to years. This open source, GIS-based landscape evolution model can simulate either steady state or unsteady flow regimes, dynamically switch between soil erosion regimes, and simulate the evolution of fine-scale morphological features such as ephemeral gullies (Figure 2). It was designed as a research tool for studying how erosional processes scale over time and space, comparing empirical and process-based models, comparing steady state and unsteady flow regimes, and studying the role of unsteady flow regimes in fine-scale morphological change. r.sim.terrain was tested with a subwatershed scale ($450\ \mathrm{m}^2$) case study and the simulations were compared against a time-series of airborne lidar surveys.

2 r.sim.terrain

The process-based, spatially distributed landscape evolution model r.sim.terrain simulates topographic changes caused by shallow, overland water flow across a range of spatiotemporal scales and soil erosion regimes using either the Simulated Water Erosion (SIMWE) model, the 3-Dimensional Revised Universal Soil Loss Equation (RUSLE 3D) model, or the Unit Stream Power Erosion Deposition (USPED) model. SIMWE is a physics-based simulation that uses a Monte Carlo path sampling method to solve the water and sediment flow equations for detachment limited, transport limited, and variable erosion-deposition soil erosion regimes (Mitas and Mitasova, 1998; Mitasova et al., 2004). With SIMWE r.sim.terrain uses the modeled flow of sediment – a function of water flow and soil detachment and transport parameters – to estimate net erosion and deposition rates. RUSLE3D is an empirical equation for estimating soil erosion rates in detachment capacity limited soil erosion regimes (Mitasova et al., 1996, 2013). With RUSLE3D r.sim.terrain uses an event-based rainfall erosivity factor, the soil erodibility factor, the land cover factor, and the 3D topographic factor (function of slope and the flow accumulation) to model soil erosion rate. USPED is an semi-empirical equation for net erosion and deposition in transport capacity limited soil erosion regimes (Mitasova et al., 1996, 2013). With USPED r.sim.terrain uses an event-based rainfall erosivity factor, the soil erodibility factor, the land cover factor, and the 3D topographic factor (function of slope and the flow accumulation) to model net erosion or deposition rates as the divergence of sediment flows. For each of the models topographic change is derived at each time step from the erosion rate or net erosion-deposition ratei, and gravitational diffusion. The r.sim.terrain model can simulate either steady state or unsteady water flow regimes. Depending on the input parameters, simulations with SIMWE r.sim.terrain can represent variable soil erosion-deposition regimes, including prevailing detachment capacity limited, or prevailing transport capacity limited regimes.

The r.sim.terrain model can simulate the evolution of gullies including processes such as knickpoint migration, channel incision, channel widening, aggradation, and scour pool and depositional ridge formation along the thalweg of the gully. Applications include geomorphological research, erosion control, landscape restoration, and scenario development for landscape planning and management. This model can simulate landscape evolution over a wide range of spatial scales from

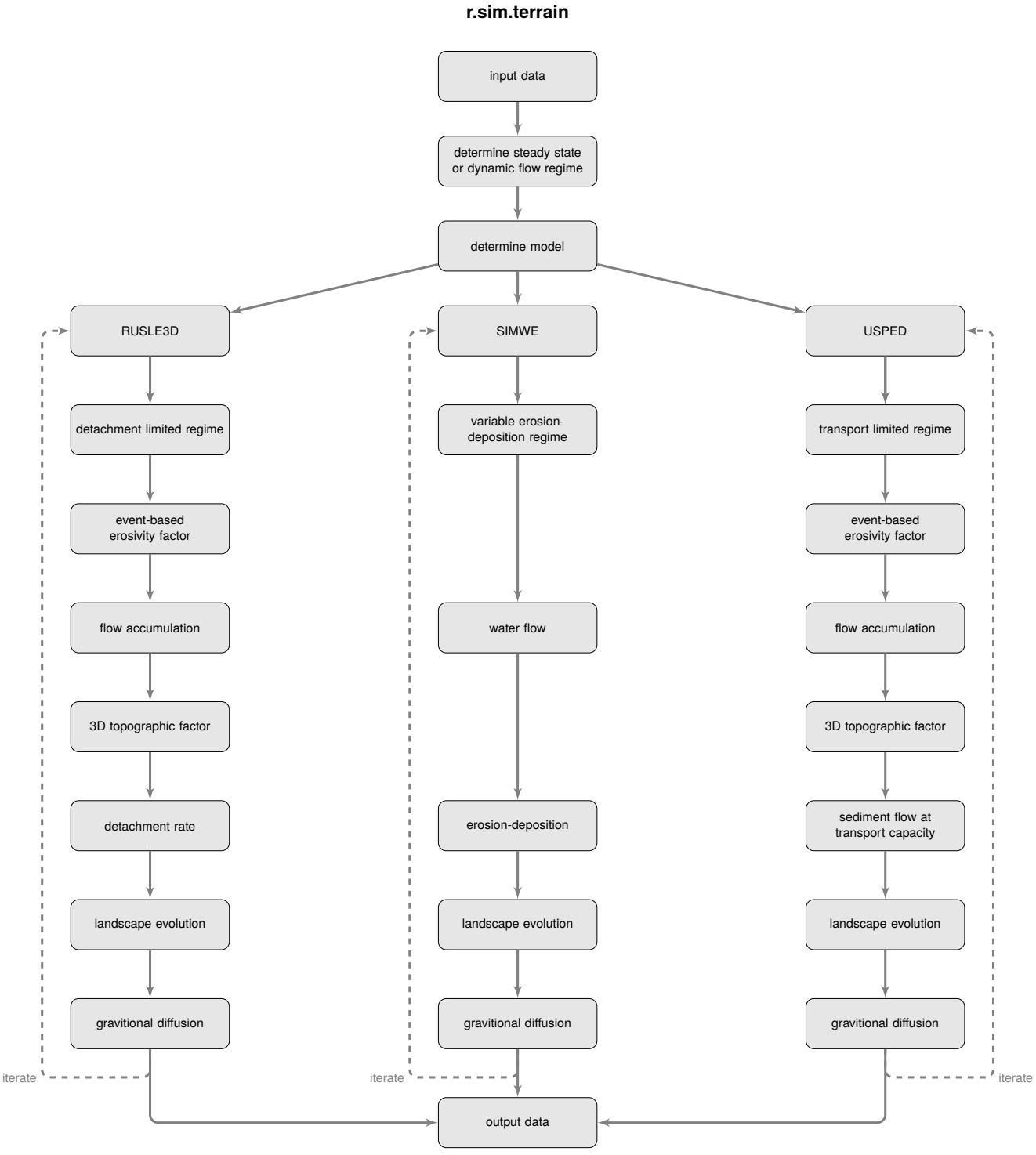

Figure 2. Conceptual diagram for r.sim.terrain. REPLACE SED FLOW BY DETACH IN RUSLE

small watersheds less than ten square kilometers with SIMWE to regional watersheds of hundreds of square kilometers with USPED or RULSE3D, although it does not model fluvial processes. It has been used at resolutions ranging from sub-meter to 30m. This model has been implemented as a Python add-on module for the free, open source Geographic Resources Analysis Support System (GRASS) GIS (GRASS Development Team). The source code is available at https://github.com/baharmon/landscape_evolution under the GNU General Public License v2. It supports multithreading and parallel processing to efficiently compute simulations using large, high resolution topographic datasets. The landscape evolution model can be installed in GRASS GIS as an add-on module with the command:

```
g.extension r.sim.terrain
```

Limitations of this landscape evolution model include shallow overland flow, units, computation time, resolution and spatial scale. r.sim.terrain only models shallow overland flows, not fluvial processes or subsurface flows. It requires data – including elevation and rainfall intensity – in metric units. The SIMWE model is computationally intensive and may require long computation times even with multithreading. Because SIMWE uses a Green's function Monte Carlo solution of the sediment transport equation, the accuracy, detail, and smoothness of the results depend on the number of random walkers. While a large number of random walkers will reduce the numerical error in the path sampling solution, it will also greatly increase computation time. Furthermore a customized compilation of GRASS GIS is needed for more than 7 million random walkers. This limits the size of the raster layers that can be processed while RUSLE3D and USPED are much faster, computationally efficient, and can easily be run for much larger rasters.

2.1 Landscape evolution

Landscape evolution in r.sim.terrain is driven by change in elevation surface caused by soil erosion and deposition. During storm events, overland flow erodes soil, transports sediment across landscape and, under favorable conditions, deposits the sediment. Gravitational diffusion, applied to the changed elevation surface, simulates smoothing effects of localized transport of soil between the events.

2.1.1 Change in elevation

Assuming negligible uplift, the change in elevation over time is described by the continuity of mass equation expressed in terms of divergence of sediment flow (Tucker et al., 2001):

$$\frac{\partial z}{\partial t} = -\nabla \cdot \mathbf{q_s} = d_s \, \rho_s^{-1} \tag{2}$$

where:

z is the elevation [m]

t is the time [s]

$\mathbf{q_s}$ is the sediment flow per unit width (vector) [$\mathrm{kg\,m^{-1}\,s^{-1}}$]

d_s is the net erosion-deposition rate [$\mathrm{kg\,m^{-2}\,s^{-1}}$]

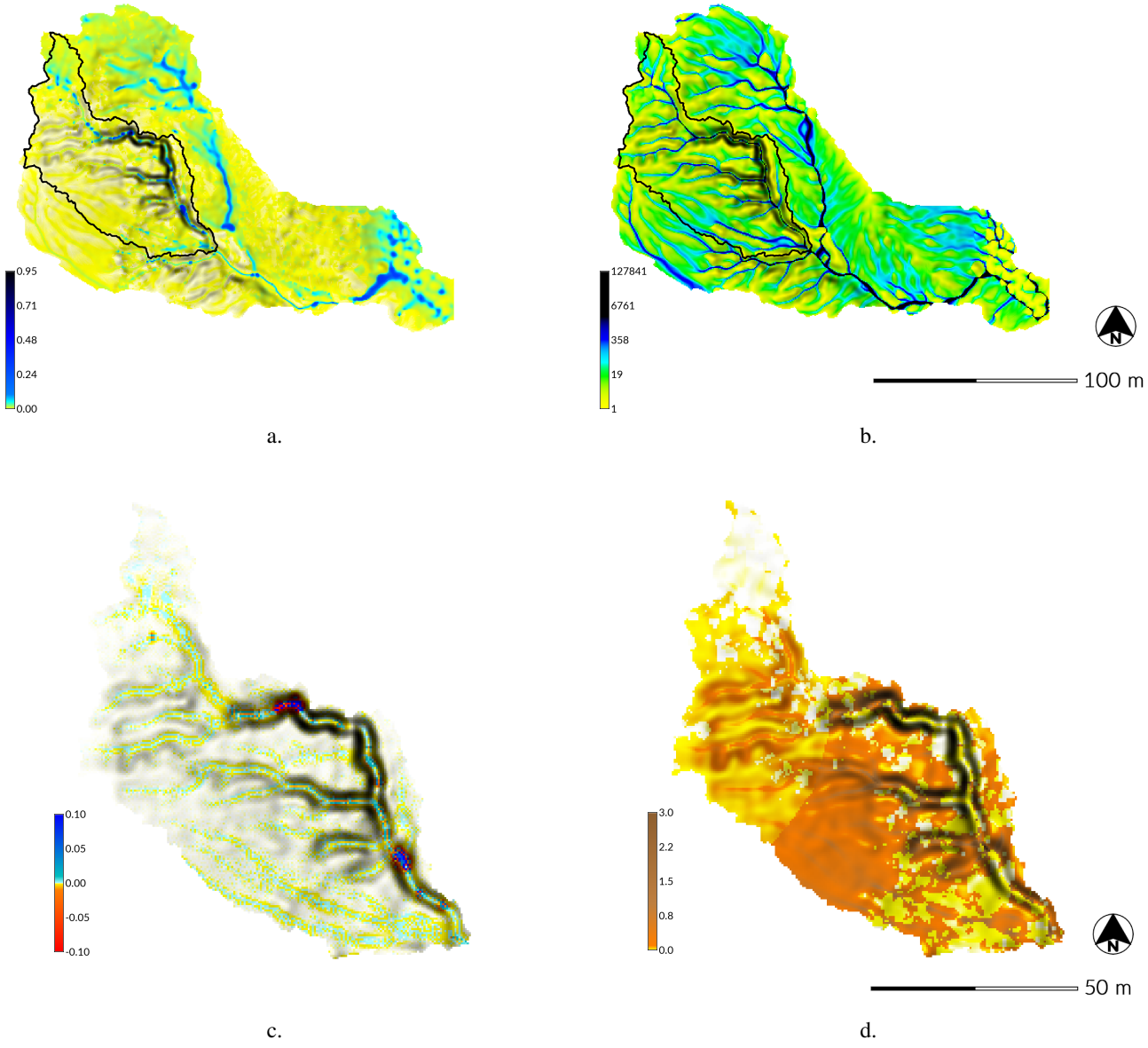

Figure 3. Water flow for a subwatershed (a, d), sediment flow and net erosion deposition (b, c) topographic erosion factor and net erosion (e,f) for drainage area 1 of Patterson Branch modeled by SIMWE for a 10 min event with 50 $\mathrm{mm\,hr^{-1}}$ (a-c) and by RUSLE3D with a R-factor of 310 UNITS??? (d-f)

ρ_s is the sediment mass density [$\mathrm{kg\,m^{-3}}$]

The overland flow driven net erosion-deposition rate d_s is in r.sim.terrain estimated at different levels of complexity based on the user selected simulation mode guided by the type of application.

Gravitational diffusion is then applied to the changed topography to simulate smoothing effects of localized transport of soil that occurs between rainfall events. The change in elevation due to gravitational diffusion is a function of the the sediment mass density, the diffusion coefficient, and Laplacian of the elevation (Thaxton, 2004):

$$\frac{\partial z}{\partial t} = \rho_s^{-1}\, \varepsilon_g\, \nabla^2 z \tag{3}$$

where ε_g is the diffusion coefficient [$\mathrm{kg\,m^2\,s^{-1}}$].

The discrete implementation follows Thaxton (2004):

$$z_{t+\Delta t_1} = z_t + \Delta z_s \tag{4}$$

$$z_{t+\Delta t_1+\Delta t_2} = z_{t+\Delta t_1} + \Delta z_g \tag{5}$$

where:

Δz_s is elevation change caused by net erosion or deposition [m], (Eq. 2)

Δz_g is the diffusion driven elevation change [m], (Eq. 3)

t is the time [s]

Δt_1 is the time interval during a storm event [s]

Δt_2 is the time interval between the events when the gravitational diffusion changes the elevation surface[s]

2.1.2 Erosion-deposition regimes

Following experimental observations and qualitative arguments, Foster et al. (1977) proposed that the ratio of net erosion-deposition rate d_s to detachment capacity D_c [$\mathrm{kg\,m^{-2}\,s^{-1}}$] plus the ratio of sediment flow rate $q_s = |\mathbf{q_s}|$ to sediment transport capacity T_c [$\mathrm{kg}\ m^{-1}\ s^{-1}$] is a conserved quantity (unity):

$$\frac{d_s}{D_c} + \frac{q_s}{T_c} = 1 \tag{6}$$

and the net erosion and deposition rate d_s can then be expressed as proportional to the difference between the sediment transport capacity T_c and the actual sediment flow rate q_s:

$$d_s = \frac{D_c}{T_c}\left(T_c - q_s\right) \tag{7}$$

This principle is used in several erosion models such as Water Erosion Prediction Project (WEPP) (Flanagan et al., 2013) or SIMWE (Mitas and Mitasova, 1998).

Using this concept it is possible to identify two limiting erosion-deposition regimes. For $T_c >> D_c$ leading to $T_c >> q_s$, the erosion regime is detachment capacity limited and net erosion is equal to the detachment capacity:

$$d_s = D_c \tag{8}$$

For this case, transport capacity of overland flow exceeds detachment capacity and consequently the sediment flow everywhere, erosion and sediment transport is limited by the detachment capacity and therefore no deposition occurs. An example of this case is a strong storm producing large overland flow over compacted clay soil leading to high capacity of flow to transport the light clay particles while the detachment of the compacted soil is limited.

For $D_c >> T_c$ the sediment flow is at sediment transport capacity $q_s = T_c$, leading to a transport capacity limited regime with deposition reaching its maximum extent for the given water flow. The net erosion-deposition is computed as a divergence of transport capacity multiplied by a unit vector $\mathbf{s_0}$ in the direction of flow:

$$d_s = \nabla \cdot (T_c\, \mathbf{s_0}) \tag{9}$$

This case may occur, for example, during a moderate storm and overland flow in areas with sandy soils with high detachment capacity but low transport capacity.

For $0 < (D_c/T_c) < \infty$ the spatial pattern of net erosion-deposition is variable and depends on the difference between the sediment transport capacity and the actual sediment flow rate at the given location.

The detachment capacity, D_c and the sediment-transport capacity T_c are estimated using shear stress and stream power equations respectively expressed as power functions of water-flow properties and slope angle. The relation between the topographic parameters of the well known empirical equations for erosion modeling, such as USLE and stream power was presented by (Moore and Burch, 1986) and used to develop simple, GIS-based models for the limiting erosion-deposition cases, including RUSLE3D and USPED (Mitasova and Mitas, 2001). The SIMWE model estimates T_c and D_c using modified equations and parameters developed for the WEPP model (Flanagan et al., 2013; Mitasova and Mitas, 2001).

The simulation modes in r.sim.terrain include

- the process-based SIMWE model for steady state and unsteady shallow overland flow and variable erosion-deposition regime with d_s computed by solving the shallow water flow and sediment transport continuity equations,
- USPED model for the transport capacity limited regime with d_s given by Eq. (9)
- RUSLE3D model for the detachment capacity limited case with d_s given by Eq. (8).

The following sections explain the computation of d_s for these three modes in more detail.

2.2 Simulation of Water Erosion (SIMWE)

SIMWE is a physics-based simulation of shallow overland water and sediment flow that uses a path sampling method to solve the continuity equations with a 2D diffusive wave approximation (Mitas and Mitasova, 1998; Mitasova et al., 2004). SIMWE

has been implemented in GRASS GIS as the modules r.sim.water and r.sim.sediment. In the SIMWE mode for each landscape evolution time step r.sim.terrain:

- computes the first order partial derivatives of elevation surface $\partial z/\partial x$ and $\partial z/\partial y$, using the GRASS GIS module r.slope.aspect (see the equations in Hofierka et al. (2009)),
- simulates shallow water flow depth, sediment flow, and net erosion-deposition rate,
- then evolves the topography based on the erosion-deposition rate and gravitational diffusion.

The model simulates unsteady-state flow regimes when the landscape evolution time step is less than the travel time for a drop of water or a particle of sediment to cross the landscape, e.g. the time step is less than the time to concentration for the modeled watershed. With longer landscape evolution time steps the model simulates a steady state regime.

2.2.1 Shallow water flow

The SIMWE model simulates shallow overland water flow controlled by spatially variable topographic, soil, landcover, and rainfall parameters by solving the water flow continuity equation using Green's function Monte Carlo path sampling method

$$\nabla \cdot \mathbf{q} = i_e \tag{10}$$

where:

i_e is the rainfall excess rate [$\mathrm{m\,s^{-1}}$] (i.e. rainfall intensity − infiltration − vegetation intercept)

$\mathbf{q}$ is the water flow per unit width (vector) [$\mathrm{m^2\ s^{-1}}$].

The path sampling method solves the continuity equation by accumulation of the evolving source over the given time period. This accumulation process can be interpreted as an approximation of a dynamical solution, with diffusive wave effects incorporated by adding a diffusion term proportional to $\nabla^2[h^{5/3}]$ into the solution (see Mitasova et al. (2004) for more details on this equation and its numerical solution):

$$-\frac{\varepsilon_w}{2}\nabla^2\, h^{5/3} + \nabla \cdot \mathbf{q} = i_e \tag{11}$$

where:

ε_w is a spatially variable diffusion coefficient [$\mathrm{m^{4/3}\ s^{-1}}$].

The solution assumes that water flow velocity is mostly controlled by terrain slope and surface roughness and its change during the simulated event at a given location is negligible. The water depth h at time τ during the simulated rainfall event is computed as function of particle (walkers) density at each grid cell. The initial number of particles per grid cell is proportinal to rainfall excess rate i_e (source) and the particles are then routed across the landscape by finding a new position of the walker at time $\tau + \Delta\tau$ by:

$$\mathbf{r}_m^{new} = \mathbf{r}_m + \Delta\tau\mathbf{v} + \mathbf{g} \tag{12}$$

where:

$\mathbf{r} = (x, y)$ is the m^{th} walker position [m]

$\Delta\tau$ is the particle routing time step [s]

$\mathbf{g}$ is a random vector with gaussian components with variance $\Delta\tau$ [m]

$\mathbf{v}$ is the water flow velocity vector [$\mathrm{m\,s^{-1}}$], with the magnitude computed by Manning equation $v = n^{-1}\ h^{2/3}\ s^{1/2}$, where n is Manning coefficient [$\mathrm{s\,m^{-1/3}}$], and s is slope

ADD COMPUTATION OF WALKER DENSITY HERE

The mathematical background of the method is presented by Mitas and Mitasova (1998); Mitasova et al. (2004), including the incoporation of approximate momentum through increased diffusion rate in the prevailing direction of flow.

2.2.2 Sediment flow and net erosion-deposition

The SIMWE model simulates the sediment flow over complex topography with spatially variable overland flow, soil and land-cover properties by solving the sediment flow continuity equation using Green's function Monte Carlo path sampling method. Steady state sediment flow $\mathbf{q_s}$ is approximated by the bivariate continuity equation which relates the change in sediment flow rate to effective sources and sinks:

$$\nabla \cdot \mathbf{q_s} = \mathrm{sources} - \mathrm{sinks} = d_s \tag{13}$$

while the sediment-flow rate $\mathbf{q_s}$ is a function of water flow and sediment concentration: (Mitas and Mitasova, 1998), (Fig. 3b):

$$\mathbf{q_s} = \rho_s\ c\ \mathbf{q} = \rho_s\ c\ h\ \mathbf{v} = \varrho\ \mathbf{v} \tag{14}$$

where:

ρ_s is sediment mass density in the water column [$\mathrm{kg\,m^{-3}}$].

c is the sediment concentration [$\mathrm{particle\,m^{-3}}$]

$\varrho = \rho_s\ c\ h$ is the mass of sediment transported by water per unit area [$\mathrm{kg\,m^{-2}}$].

Similarly as for the water flow, the sediment flow equation (13) is rewritten to include a small diffusion term proportional to the mass of water-carried sediment per unit area $\nabla^2\varrho$ (Mitas and Mitasova, 1998):

$$-\frac{\varepsilon_s}{2}\nabla^2\varrho + \nabla\cdot[\varrho\mathbf{v}] + \varrho\ \frac{D_c}{T_c}\ |\mathbf{v}| = D_c \tag{15}$$

where:

ε_s is the diffusion constant [$\mathrm{m^2\,s^{-1}}$]

On the left hand side of the equation (15), the first term describes local diffusion, the second term is a drift driven by the water flow while the third term represents a velocity dependent 'potential' acting on the mass of transported sediment. The

initial number of particles per grid cell is proportinal to the soil detachment capacity D_c (source) and the particles are then routed across the landscape by finding a new position of the walker at time $\tau + \Delta\tau$ as:

$$\mathbf{r}_m^{new} = \mathbf{r}_m + \Delta\tau \mathbf{v} + \mathbf{g} \tag{16}$$

while the updated weight is:

$$w_m^{new} = w_m \exp[-\Delta\tau(u(\mathbf{r}_m^{new}) + u(\mathbf{r}_m))/2] \tag{17}$$

where $u = D_c/T_c\ |\mathbf{v}|$. The sediment flow rate is then computed as weighted particle densities multiplied by unit vector in the direction of flow VERIFY $\mathbf{q_s} = \varrho\ \mathbf{s_0}$ and then net erosion-deposition d_s is computed as divergence of sediment flow using equation (13).

SIMWE estimates the detachment capacity D_c, and the sediment-transport capacity T_c as functions of shear stress and stream power respectively.

Specifically, the detachment capacity is:

$$D_c = K_d\big(\gamma - \gamma_0\big)^b \tag{18}$$

where:

K_d is the effective erodibility (detachment-capacity coefficient) [$\mathrm{s\,m^{-1}}$] for $b = 1$ VERIFY

$\gamma = \rho_w\ g\ h\ \sin\beta$ is the shear stress [$\mathrm{Pa = kg\,m^{-2}}$]

ρ_w is the mass density of water [$\mathrm{kg\,m^{-3}}$]

g is the gravitational acceleration [$\mathrm{m\,s^{-2}}$]

γ_0 is the critical shear stress [Pa]

b is an empirical exponent. The shear stress, γ, is computed as a function water depth h estimated by r.sim.water and surface slope angle, $\beta[deg]$.

Sediment-transport capacity is computed as a function of the unit stream power ω (Moore and Burch, 1986):

$$T_c = K_s\omega = K_s\ \gamma\ |\mathbf{v}| = K_s\ n^{-1}\ g_w\ h^m\ (\sin\beta)^p, \tag{19}$$

where:

K_s is the effective sediment-transport capacity coefficient [s]

m and p is an empirical exponent CHECK implementation may have omega just power of gamma without velocity

This model can simulate erosion regimes from prevailing detachment limited when $T_c >> D_c$ to prevailing transport capacity limited when $D_c >> T_c$ and the erosion-deposition patterns in-between. At each landscape evolution time step, the regime can change based on the ratio between the sediment detachment capacity D_c, and the sediment transport capacity T_c and the actual sediment flow rate. If the landscape evolution time step is shorter than time to concentration (time for water to reach steady state) the net erosion-deposition is derived from unsteady flow.

2.3 Revised Universal Soil Loss Equation for Complex Terrain (RUSLE3D)

RUSLE3D is an empirical model for computing erosion in a detachment capacity limited soil erosion regime for watersheds with complex topography (Mitasova et al., 1996). It is based on the Universal Soil Loss Equation (USLE), an empirical equation for estimating the average sheet and rill soil erosion from rainfall and runoff on agricultural fields and rangelands with simple topography (Wischmeier et al., 1978). It models erosion dominated regimes without deposition in which sediment transport capacity is uniformly greater than detachment capacity. In USLE soil loss per unit area is determined by an erosivity factor R, a soil erodibility factor K, a slope length factor L, a slope steepness factor S, a cover management factor C, and a prevention measures factor P. These factors are empirical constants derived from an extensive collection of measurements on $22.13\ \mathrm{m}$ standard plots with an average slope of 9%. RUSLE3D was designed to account for more complex, 3D topography with converging and diverging flows. In RUSLE3D the topographic potential for erosion at any given point is represented by a 3D topographic factor LS_{3D}, which is a function of the upslope contributing area and the angle of the slope.

In this spatially and temporally distributed model RUSLE3D is modified by the use of a event-based R-factor derived from the rainfall intensity at each time step. For each time step this model computes the parameters for RUSLE3D – an event-based erosivity factor, the slope of the topography, the flow accumulation, and the 3D topographic factor – and then computes the RUSLE3D equation for soil loss rate (net soil erosion rate). The soil erosion rate rate is used to simulate landscape evolution in a detachment capacity limited soil erosion regime.

2.3.1 Event-based erosivity factor

The erosivity factor R in USLE and RUSLE is the combination of the total energy and peak intensity of a rainfall event, representing the interaction between the detachment of sediment particles and the transport capacity of the flow. It can be calculated as the product of the the kinetic energy of the rainfall event E and its maximum 30 min intensity I_{30} (Brown and Foster, 1987; Renard et al., 1997). In this model, however, the erosivity factor is derived at each time step as a function of kinetic energy, rainfall depth, rainfall intensity, and time. First rain energy is derived from rainfall intensity (Brown and Foster, 1987; Yin et al., 2017):

$$\frac{e_r}{e_0} = 1. - b\ exp(\frac{i_r}{i_0}) \tag{20}$$

where:

$e_r$is unit rain energy [$\mathrm{MJ\,ha^{-1}\ mm^{-}1}$]

i_r is rainfall intensity [$\mathrm{mm\,h^{-1}}$]

b is empirical coeficient

i_0 is reference rainfall intensity [$\mathrm{mm\,h^{-1}}$]

e_0 is reference energy [$\mathrm{MJ\,ha^{-1}\ mm^{-}1}$] The parameters for this equation were derived from observed data and published for different regions by...

Then the event-based erosivity index R_e is calculated as the product of unit rain energy, rainfall depth, rainfall intensity, and time:

$$R_e = e_r \; v_r \; i_r \; t_r \tag{21}$$

where:

R_e is the event-based erosivity index [$\mathrm{MJ\,mm\,ha^{-1}\,hr^{-1}}$]

v_r is the rainfall depth [mm] derived from $v_r = i_r \; t_r$

t_r is the time interval [s].

2.3.2 Flow accumulation

The upslope contributing area per unit width a is determined by flow accumulation (number of grid cells draining into a given grid cell) multiplied by grid cell width (Fig. 3d). Flow accumulation is calculated using a multiple flow direction algorithm (Metz et al., 2009) based on A^T least cost path searches (Ehlschlaeger, 1989). The multiple flow direction algorithm implemented in GRASS GIS as the module r.watershed is computationally efficient, does not require sink filling and can navigate nested depressions and other obstacles.

2.3.3 3D topographic factor

The 3D topographic factor LS_{3D} is calculated as a function of upslope contributing area and the slope (Fig. 3e).

$$LS_{3D} = (m+1) \left(\frac{a}{a_0}\right)^m \left(\frac{\sin\beta}{\beta_0}\right)^n \tag{22}$$

where:

LS_{3D} is the dimensionless topographic factor

a is upslope contributing area per unit width [m]

a_0 is the length of the standard USLE plot [22.1 m]

β is the angle of the slope [$^\circ$]

m is an empirical coefficient

n is an empirical coefficient

β_0 is the slope of the standard USLE plot [0.09°]

The empirical coefficients m and n for the upslope contributing area and the slope can range from 0.2 to 0.6 and 1.0 to 1.3 respectively with low values representing dominant sheet flow and high values representing dominant rill flow.

2.3.4 Detachment limited erosion rate

Erosion rate is a function of the event-based erosivity factor, the soil erodibility factor, the 3D topographic factor, cover factor, and the prevention measures factor (Fig. 3f):

$$E = R_e \; K \; LS_{3D} \; C \; P \tag{23}$$

where:

E is soil erosion rate (soil loss) [$\mathrm{kg\,m^{-2}\,min^{-1}}$]

R_e is the event-based erosivity factor [$\mathrm{MJ\,mm\,ha^{-1}\,hr^{-1}}$]

K is the soil erodibility factor [$\mathrm{ton\,ha\,hr\,ha^{-1}\,MJ^{-1}\,mm^{-1}}$]

LS_{3D} is the dimensionless topographic (length-slope) factor

C is the dimensionless land cover factor

P is the dimensionless prevention measures factor.

The detachment limited erosion represented by RUSLE3D leads to the simulated change in elevation:

$$\Delta z_s = D_c \rho_s^{-1} = E\ \rho_s^{-1} \tag{24}$$

which is combined with Eq. (3) for gravitational diffusion.

2.4 Unit Streampower Erosion Deposition (USPED)

USPED estimates net erosion-deposition as the divergence of sediment flow in transport capacity limited soil erosion regime. At transport capacity shallow flows of water are carrying as much sediment as possible IF THIS WAS TRUE THERE WOUL BE DEPOSITION EVERWHERE - REMOVE – more sediment is being detached than can be transported. WE CAN WRITE: The amount of soil detached is close to the amount of sediment that water flow can cary. As a transport capacity limited model USPED predicts erosion where transport capacity increases and deposition where transport capacity decreases. The influence of topography on sediment flow is represented by a topographic sediment transport factor, while the influence of soil and landcover are represented by factors adopted from USLE and RUSLE (Mitasova et al., 1996). The sediment flow is estimated by computing the event-based erosivity factor (R_e) using Eq. 21, the slope and aspect of the topography, the flow accumulation with a multiple flow direction algorithm, the topographic sediment transport factor, and the sediment flow at transport capacity. The net erosion-deposition is then computed as the divergence of the sediment flow.

Using the unit stream power concept presented by Moore and Burch (1986), the 3D topographic factor (Eq. 22) for RUSLE3D is modified to represent the topographic sediment transport factor (LS_T) – the topographic component of overland flow at sediment transport capacity:

$$LS_T = a^m\ (\sin\beta)^n \tag{25}$$

where:

LS_T is the topographic sediment transport factor

a is the upslope contributing area per unit width [m]

β is the angle of the slope [$^\circ$]

m is an empirical coefficient

n is an empirical coefficient.

The sediment flow at transport capacity is a function of the event-based rainfall factor, the soil erodibility factor, the topographic component of overland flow, the landcover factor, and the prevention measures factor:

$$T = R_e\ K\ C\ P\ LS_T \tag{26}$$

where:

T is sediment flow at transport capacity [$\mathrm{kg\,m^{-1}\,s^{-1}}$]

R_e is the event-based rainfall factor [$\mathrm{MJ\,mm\,ha^{-1}\,hr^{-1}}$]

K is the soil erodibility factor [$\mathrm{ton\,ha\,hr\,ha^{-1}\,MJ^{-1}\,mm^{-1}}$]

C is the dimensionless land cover factor

P is the dimensionless prevention measures factor.

Net erosion-deposition is estimated as the divergence of sediment flow, assuming that the sediment flow is equal sediment transport capacity:

$$d_s = \frac{\partial(T\ \cos\alpha)}{\partial x} + \frac{\partial(T\ \sin\alpha)}{\partial y} \tag{27}$$

where:

d_s is net erosion-deposition [$\mathrm{kg\,m^{-2}\,s^{-1}}$]

α is the aspect of the topography (direction of flow) [$^\circ$].

UPDATE based on the new structure of the paper With USPED the simulated change in elevation $\Delta z_s = d_s$ is derived from equation 2 for landscape evolution and then equation 3 for the gravitational diffusion.

3 Case study

Military activity is a high-impact land use that can cause significant physical alteration to the landscape. Erosion is a major concern for military installations, particularly at training bases, where the land surface is disturbed by off-road vehicles, foot traffic, and munitions. Off-road vehicles and foot traffic by soldiers cause the loss of vegetative cover, the disruption of soil structure, soil compaction, and increased runoff due to reduced soil capacity for water infiltration (Webb and Wilshire, 1983; McDonald, 2004). Gullies – ephemeral channels with steep headwalls that incise into unconsolidated soil to depths of meters – are a manifestation of erosion common to military training installations like Ft. Bragg in North Carolina and the Piñon Canyon Maneuver Site in Colorado. While the local development of gullies can restrict the maneuverability of troops and vehicles during training exercises, pervasive gullying across a landscape can degrade an entire training area (Huang and Niemann, 2014).

To test the effectiveness of the different models in r.sim.terrain we compared the simulated evolution of a highly eroded subwatershed of Patterson Branch on Fort Bragg, North Carolina against a timeseries of airborne lidar surveys. The models –

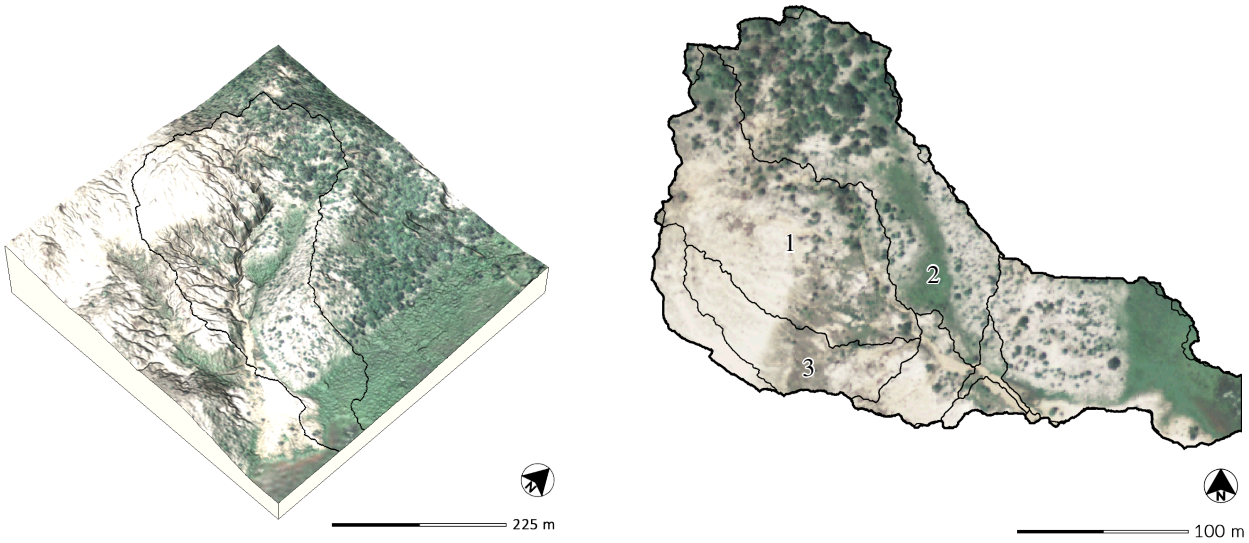

a. b.

Figure 4. Subwatershed with 2014 orthoimagery draped over the 2016 digital elevation model (a) and drainage areas with 2014 orthoimagery (b), Patterson Branch, Fort Bragg, NC, USA

SIMWE, RUSLE3D, and USPED – were tested in steady state and dynamic modes for constant rainfall, design storms, and recorded rainfall.

3.1 Patterson Branch

With 650 km^2 of land Fort Bragg is the largest military installation in the US and has extensive areas of bare, erodible soils on impact areas, firing ranges, landing zones, and dropzones. It is located in the Sandhills region of North Carolina with a Longleaf Pine and Wiregrass Ecosystem (Sorrie et al., 2006). The study landscape – a subwatershed of Patterson Branch (Figure 4a) in the Coleman Impact Area – is pitted with impact craters from artillery and mortar shells and has an active, approximately 2 m deep gully. It is a Pine-Scrub Oak Sandhill community composed primarily of Longleaf Pine (*Pinus palustris*) and Wiregrass (*Aristida stricta*) on Blaney and Gilead loamy sands (Sorrie, 2004). Throughout the Coleman Impact Area frequent fires ignited by live munitions drive the ecological disturbance regime of this fire adapted ecosystem. In 2016 the 450 m^2 study site was 43.24% bare ground with predominately loamy sands, 39.54% covered by the Wiregrass community, and 17.22% forested with the Longleaf Pine community (Figure 5a). We hypothesize that the elimination of forest cover in the impact zone triggered extensive channelized overland flow, gully formation, and sediment transport into the creek.

Timeseries of digital elevations models and landcover maps for the study landscape were generated from lidar pointclouds and orthophotography. The digital elevations models for 2004, 2012, and 2016 were interpolated at 0.3 m resolution using

the regularized spline with tension function (Mitasova and Mitas, 1993; Mitasova et al., 2005) from airborne lidar surveys collected by the NC Floodplain Mapping program and Fort Bragg. Unsupervised image classification was used to identify clusters of spectral reflectance in a timeseries of 1 m resolution orthoimagery collected by the National Agriculture Imagery Program. The landcover maps were derived from the classified lidar point clouds and the classified orthoimagery. Spatially variable soil erosion factors – k-factor, c-factor, Manning coefficient, and runoff rates – were then derived from the landcover and soil maps. The dataset for this study is hosted at https://github.com/baharmon/landscape_evolution_dataset under the ODC Open Database License (ODbL). The data is derived from publicly available data from the US Army, USGS, USDA, Wake County GIS, NC Floodplain Mapping Program, and the NC State Climate Office. There are detailed instructions for preparing the input data in the tutorial and a complete record of the commands used to process the sample data in the data log.

We used the geomorphons method of automated landform classification based on the openness of terrain (Jasiewicz and Stepinski, 2013) and the difference between the digital elevation models to analyze the changing morphology of the study area (Figure 5c-d). The 2 m deep gully – its channels classified as valleys and its scour pits as depressions by geomorphons – has multiple mature branches and ends with a depositional fan. The gully has also developed depositional ridges beside the channels. Deep scour pits have developed where branches join the main channel and where the main channel has sharp bends. A new branch has begun to form in a knickzone classified as a mix of valleys and hollows on a grassy swale on the northeast side of the gully. Between 2012 and 2016 a depositional ridge has developed at the foot of this nascent branch where it would meet the main channel. The difference in elevation between 2012 and 2016 (Figure 5b) shows a deepening of the main channel by approximately 0.2 m and the scours pits by approximately 1 m, while depositional ridges have formed and grown up to approximately 1 m or more.

3.2 Simulations

We ran a sequence of r.sim.terrain simulations with design storms for the Patterson Branch subwatershed study area to test and demonstrate the capabilities of the RUSLE3D, USPED, and SIMWE models (Table **??**). Since the study area was dominated by a variable erosion-deposition or transport limited soil erosion regime during the 2012-2016 study period, we could not quantitatively assess the detachment capacity limited models against the observed topographic evolution of the landscape. Instead the goal of simulations was to test what morphological processes and features the different models could simulate. We analyzed the results of the simulations by qualitatively comparing landforms and the net difference in elevation and by quantitatively comparing linear regressions of elevation change.

While r.sim.terrain can use rainfall records, we used design storms to demonstrate and test the basic capabilities of the model. Our design storms are based off the peak rainfall values in records from the State Climate Office of North Carolina. We used RUSLE3D to simulate landscape evolution in a dynamic, detachment capacity limited soil erosion regime for a 120 min design storm with 3 min intervals and a constant rainfall intensity of 50 $\mathrm{mm\,hr^{-1}}$ (Figure 6a-b). We used USPED to simulate landscape evolution in a dynamic, transport capacity limited soil erosion regime for a 120 min design storm with 3 min intervals and a constant rainfall intensity of 50 $\mathrm{mm\,hr^{-1}}$ (Figure 6c-d). We used SIMWE to simulate landscape evolution in a steady state, variable erosion-deposition soil erosion regime for a 120 min design storm with a constant rainfall intensity

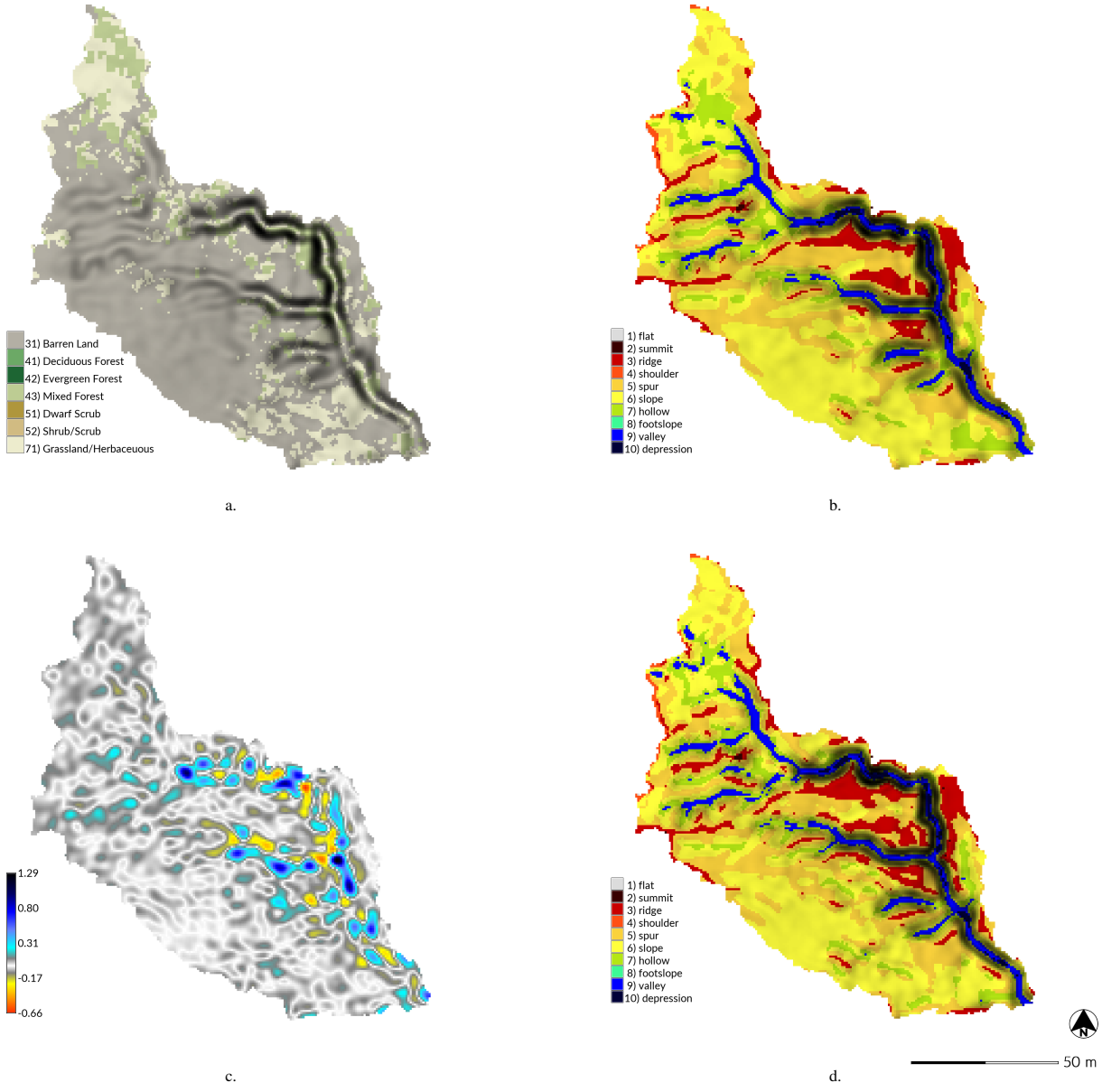

Figure 5. Morphological Change, Drainage Area 1, Study Subwatershed, Patterson Branch, Fort Bragg, NC, USA

of 50 $\mathrm{mm\,hr^{-1}}$ (Figure 7a-b). We also used SIMWE to simulate landscape evolution in a steady state, detachment capacity limited soil erosion regime for a 120 min design storm with a constant rainfall intensity of 25 $\mathrm{mm\,hr^{-1}}$ (Figure 7c-d). We used a lower rainfall intensity for this simulation to reduce overshoot. In all of the simulations a sink filling algorithm – an optional parameter in r.sim.terrain – was used to reduce the effects of positive feedback loops that cause the over-development of scour pits.

The simulations were automated and run in parallel using Python scripts that are available in the software repository. The simulations can be reproduced using these scripts and the study area dataset by following the instructions in the Open Science Framework repository at https://osf.io/tf6yb/. The simulations were run in GRASS GIS 7.4 on a desktop computer with 64-bit Ubuntu 16.04.4 LTS, 8 x 4.20 GHz Intel Core i7 7700K CPUs, and 32 GB RAM. Simulations using SIMWE are far more computationally intensive than RULSE3D or USPED, but support multi-threading when compiled with OpenMP. Dynamic simulations of RUSLE3D and USPED each took 3 min 14 s to run on a single thread, while steady state simulations for SIMWE each took 84 min 13 s running on 6 threads (Table **??**).

3.3 Results

We used linear regression to quantitatively analyze observed versus simulated changes in topographic elevation (Table **??**). As expected given that the gully was dominated by a variable erosion-deposition or transport capacity limited soil erosion regime throughout the study period, the detachment capacity limited models diverged more from the 2012-2016 baseline.

The dynamic RUSLE3D simulation deepened the main channel of the gully, while the dynamic USPED simulation eroded the banks of the gully and deposited in channels causing the gully grow wider and shallower (Figure 6). As a detachment capacity limited model RUSLE3D's results were dominated by erosion and thus negative elevation change. RUSLE3D carved a deep incision in the main gully channel where water and sediment flow accumulated (Figure 6c). As a transport capacity limited model USPED generated a distributed pattern with both erosion and deposition and thus negative and positive elevation change. While USPED's pattern of elevation change was grainy and fragmented, it captured the process of channel filling and widening expected with a transport capacity limited soil erosion regime (Figure 6f).

The steady state SIMWE simulations predicted more realistic morphological patterns of landscape evolution (Figure 7). For transport limited and variable erosion-deposition regimes SIMWE simulated channel widening and the formation of depositional ridges along the thalweg of the channel (Figure 7c). For a detachment limited soil erosion regime SIMWE simulated major erosion driving the continued development of the gully network including the spread of rills and the evolution of the nascent branch into a full fledged channel (Figure 7f). The detachment limited simulation also formed extensive ridges beside the gully channels (Figure 7f), continuing the development of channel-side ridges observed in the 2012 and 2016 landform maps (Figure 5e-f).

Given the presence the mature gully with ridges along its banks, this landscape had previously been dominated by a detachment limited soil erosion regime. The detachment limited SIMWE simulation generated the morphological features – the deeply incised gully channels, scour pits, and ridges along the channels – characteristic of a detachment-limited erosion regime, realistically simulating landscape evolution at the scale of a subwatershed. The erosion-deposition and transport lim-

ited SIMWE simulations also generated the morphological processes and features that would be expected in these regimes – gradual aggradation and the formation of a depositional ridge along the thalweg of the channel.

While RUSLE3D and USPED produced less realistic patterns of landscape evolution than SIMWE, these models were much faster and still generated the key morphological patterns and processes – channel incision, filling, and widening. Given their speed and approximate modeling of erosive processes, RUSLE3D and USPED are effective for simulating landscape evolution at regional scales, i.e. for landscapes greater than 10 km^2. RUSLE3D for example has been used to model erosion for the entire 650 km^2 Fort Bragg installation at 9 m resolution (Levine et al., 2018).

4 Conclusions

The short-term landscape evolution model r.sim.terrain can realistically simulate the development of gullies, rills, and hillslopes by overland water erosion for a range of hydrologic and soil erosion regimes. The landscape evolution model was tested with a series of simulations for different hydrologic and soil erosion regimes for a highly eroded sub-watershed on Fort Bragg with an active gully. For each regime it generated the morphological processes and features expected. The physics-based SIMWE model realistically simulated short-term topographic change for steady state hydrologic regimes at sub-watershed to watershed scales. For detachment limited soil erosion regimes it simulated morphological processes including channel incision, channel widening, and the development of knickzones, rills, and scour pits. For transport limited and variable erosion-deposition regimes, it simulated processes such as channel aggradation, scouring, and the development of depositional ridges along the thalweg. The empirical RUSLE3D and USPED models approximated short-term topographic change at watershed to regional scales. For detachment limited soil erosion regimes RUSLE3D simulated channel incision, while for transport limited regimes USPED simulated channel widening and filling. Since it is a GIS-based model that realistically simulates fine-scale morphological processes and features, r.sim.terrain can easily and effectively be used in conjunction with other GIS-based tools for geomorphological research, land management and conservation, erosion control, and landscape restoration.

In the future we plan to assess this model by comparing simulations against a monthly timeseries of submeter resolution surveys by unmanned aerial systems and terrestrial lidar. We also plan to develop a case study demonstrating how the model can be used as a planning tool for landscape restoration. Planned enhancements to model include modeling subsurface flows, accounting for bedrock, and a reverse landscape evolution mode for backward modeling.

Code and data availability. As a work of open science this study is reproducible, repeatable, and recomputable. Since the data, model, GIS, dependencies are all free and open source, the study can easily be reproduced. The landscape evolution model has been implemented in Python as module for GRASS GIS, a free and open source GIS. The source code for the model is hosted on GitHub at https://github.com/baharmon/landscape_evolution under the GNU General Public License version 2. The code repository also includes Python scripts for running and reproducing the simulations in this paper. The digital object identifier (DOI) for the version of the software documented in this paper is: https://doi.org/10.5281/zenodo.2542921. There are detailed instructions for running this model in the manual at https://grass.osgeo.org/grass76/manuals/addons/r.sim.terrain.html and the tutorial at https://github.com/baharmon/landscape_evolution/blob/master/tutorial.md.

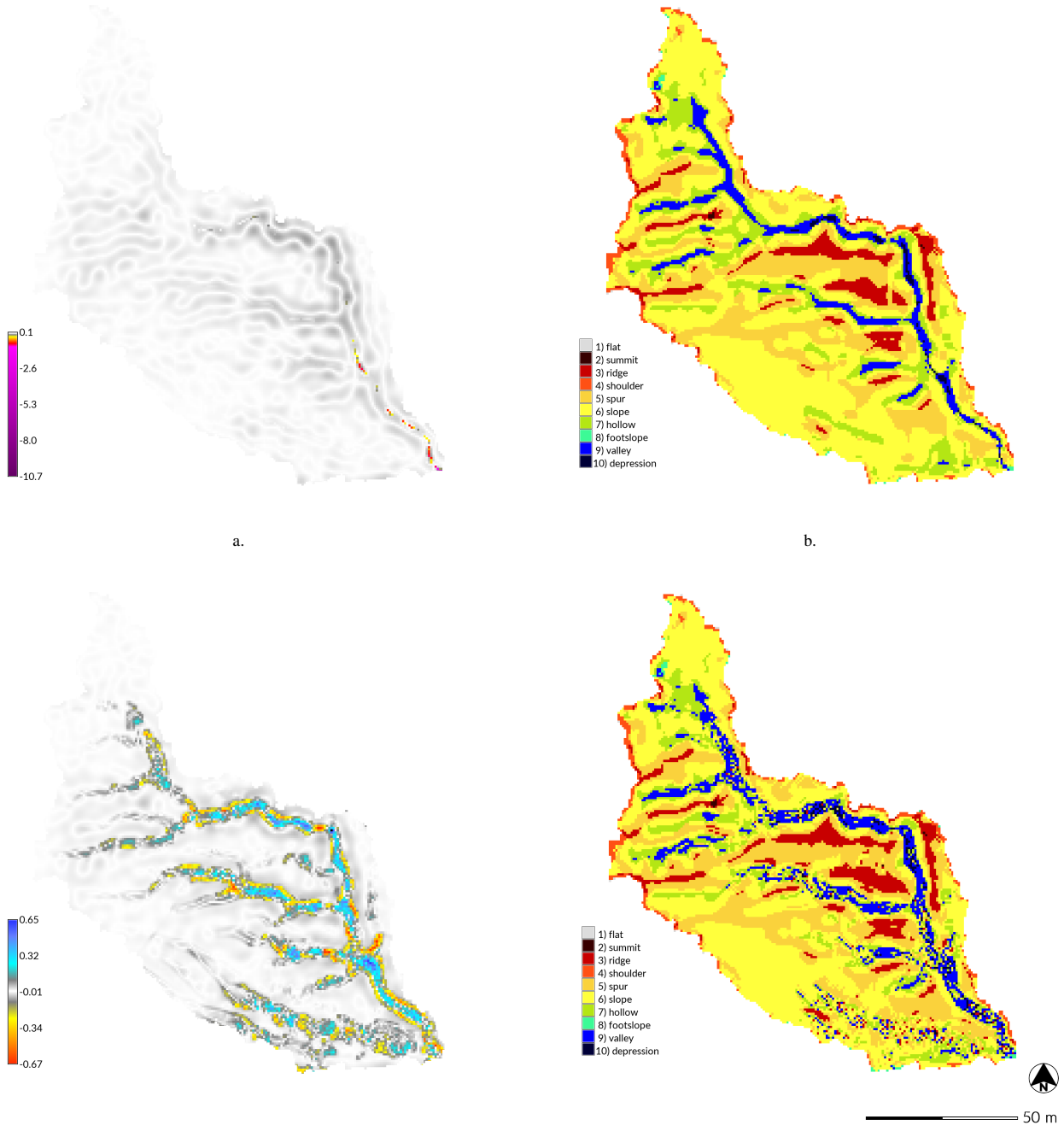

Figure 6. Dynamic RUSLE3D (a-b) and USPED (c-d) simulations for a 120 min event with a rainfall intensity of 50 $\mathrm{mm\,hr^{-1}}$, Drainage Area 1, Study Subwatershed, Patterson Branch, Fort Bragg, NC

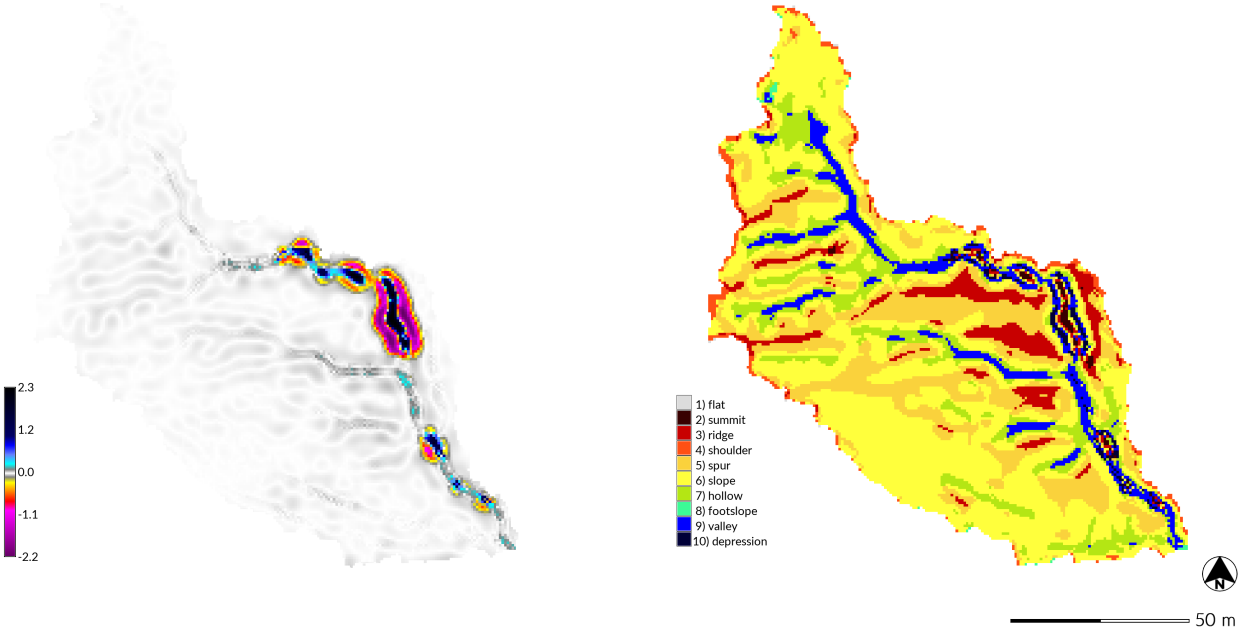

a. b.

Figure 7. Steady state SIMWE simulations for 120 min events with rainfall intensities of 50 $\mathrm{mm\ hr^{-1}}$ (a-b) and 25 $\mathrm{mm\ hr^{-1}}$ (c-d), Drainage Area 1, Study Subwatershed, Patterson Branch, Fort Bragg, NC

The geospatial dataset for the study area is available on GitHub at https://github.com/baharmon/landscape_evolution_dataset under the Open Database License with the DOI: https://doi.org/10.5281/zenodo.2542929. The data log has a complete record of the commands used to process the sample data. The source code, scripts, data, and results are also hosted on the Open Science Framework at https://osf.io/tf6yb/ with the DOI: https://doi.org/10.17605/osf.io/tf6yb.

Author contributions. Brendan Harmon developed the models, code, data, case studies, and manuscript. Helena Mitasova contributed to the development of the models and case studies and revised the manuscript. Anna Petrasova and Vaclav Petras contributed to the development of the code. All authors read and approved the final manuscript.

Competing interests. The authors declare that they have no conflict of interest.

Acknowledgements. We acknowledge the GRASS GIS Development Community for developing and maintaining GRASS GIS.

References

Barton, C. M., Ullah, I., and Mitasova, H.: Computational Modeling and Neolithic Socioecological Dynamics: a Case Study from Southwest Asia, American Antiquity, 75, 364–386, http://www.jstor.org/stable/25766199, 2010.

Bechet, J., Duc, J., Loye, A., Jaboyedoff, M., Mathys, N., Malet, J. P., Klotz, S., Le Bouteiller, C., Rudaz, B., and Travelletti, J.: Detection of seasonal cycles of erosion processes in a black marl gully from a time series of high-resolution digital elevation models (DEMs), Earth Surface Dynamics, 4, 781–798, https://doi.org/10.5194/esurf-4-781-2016, 2016.

Brown, L. C. and Foster, G. R.: Storm Erosivity Using Idealized Intensity Distributions, Transactions of the American Society of Agricultural Engineers, 30, 0379 –0386, https://doi.org/http://dx.doi.org/10.13031/2013.31957, 1987.

Dabney, S., Vieira, D., Bingner, R., Yoder, D., and Altinakar, M.: Modeling Agricultural Sheet , Rill and Ephemeral Gully Erosion, in: ICHE 2014. Proceedings of the 11th International Conference on Hydroscience & Engineering, pp. 1119–1126, Karlsruhe, 2014.

Ehlschlaeger, C.: Using the A^T Search Algorithm to Develop Hydrologic Models from Digital Elevation Data, in: Proceedings of International Geographic Information Systems (IGIS) Symposium '89, pp. 275–281, Baltimore, MD, 1989.

Flanagan, D. C., Frankenberger, J. R., Cochrane, T. A., Renschler, C. S., and Elliot, W. J.: Geospatial Application of the Water Erosion Prediction Project (WEPP) Model, Transactions of the ASABE, 56, 591–601, https://doi.org/10.13031/2013.42681, https://www.fs.usda.gov/treesearch/pubs/43830, 2013.

Foster, G., Meyer, L., and Onstad, C.: An erosion equation derived from basic erosion principles, Transactions of the American Society of Agricultural Engineers, 20, 1977.

GRASS Development Team: GRASS GIS, https://grass.osgeo.org.

Hobley, D. E., Adams, J. M., Siddhartha Nudurupati, S., Hutton, E. W., Gasparini, N. M., Istanbulluoglu, E., and Tucker, G. E.: Creative computing with Landlab: An open-source toolkit for building, coupling, and exploring two-dimensional numerical models of Earth-surface dynamics, Earth Surface Dynamics, 5, 21–46, https://doi.org/10.5194/esurf-5-21-2017, 2017.

Hofierka, J., Mitášová, H., and Neteler, M.: Geomorphometry in GRASS GIS, in: Geomorphometry, edited by Hengl, T. and Reuter, H. I., vol. 33 of *Developments in Soil Science*, pp. 387 – 410, Elsevier, https://doi.org/https://doi.org/10.1016/S0166-2481(08)00017-2, http://www.sciencedirect.com/science/article/pii/S0166248108000172, 2009.

Huang, X. and Niemann, J. D.: Simulating the impacts of small convective storms and channel transmission losses on gully evolution, in: Military Geosciences in the Twenty-First Century, edited by Harmon, R. S., Baker, S. E., and McDonald, E. V., Geological Society of America, https://doi.org/10.1007/978-1-4020-3105-2_18, 2014.

Jasiewicz, J. and Stepinski, T. F.: Geomorphons - a pattern recognition approach to classification and mapping of landforms, Geomorphology, 182, 147–156, https://doi.org/10.1016/j.geomorph.2012.11.005, 2013.

Koco, Š.: Simulation of gully erosion using the SIMWE model and GIS, Landsurface Analysis, 17, 81–86, 2011.

Levine, J., Wegmann, K., Mitasova, H., Eads, C., Lyons, N., Harmon, B., McCarther, C., Peart, S., Oberle, N., and Walter, M.: Freshwater Bivalve Survey for Endangered Species Branch Fort Bragg, NC, Tech. rep., North Carolina State University, Raleigh, NC, https://doi.org/10.13140/RG.2.2.17512.11521, 2018.

Malik, I.: Dating of small gully formation and establishing erosion rates in old gullies under forest by means of anatomical changes in exposed tree roots (Southern Poland), Geomorphology, 93, 421–436, https://doi.org/10.1016/j.geomorph.2007.03.007, 2008.

McDonald, K. W.: Military Foot Traffic Impact on Soil Compaction Properties, pp. 229–242, Springer Netherlands, Dordrecht, https://doi.org/10.1007/978-1-4020-3105-2_18, 2004.

Metz, M., Mitasova, H., and Harmon, R. S.: Fast Stream Extraction from Large , Radar- Based Elevation Models with Variable Level of Detail, pp. 237–242, 2009.

Mitas, L. and Mitasova, H.: Distributed soil erosion simulation for effective erosion prevention, Water Resources Research, 34, 505–516, https://doi.org/10.1029/97wr03347, 1998.

Mitasova, H. and Mitas, L.: Interpolation by regularized spline with tension: I. Theory and implementation, Mathematical Geology, 25, 641–655, https://doi.org/10.1007/BF00893171, 1993.

Mitasova, H. and Mitas, L.: Multiscale soil erosion simulations for land use management, in: Landscape erosion and evolution modeling, edited by Harmon, R. S. and Doe, W. W., chap. 11, pp. 321–347, Springer, Boston, MA, https://doi.org/10.1007/978-1-4615-0575-4_11, 2001.

Mitasova, H., Hofierka, J., Zlocha, M., and Iverson, L. R.: Modelling topographic potential for erosion and deposition using GIS, International Journal of Geographical Information Science, 10, 629–641, https://doi.org/10.1080/02693799608902101, http://dx.doi.org/10.1080/02693799608902101, 1996.

Mitasova, H., Thaxton, C., Hofierka, J., McLaughlin, R., Moore, A., and Mitas, L.: Path sampling method for modeling overland water flow, sediment transport, and short term terrain evolution in Open Source GIS, Developments in Water Science, 55, 1479–1490, https://doi.org/10.1016/S0167-5648(04)80159-X, 2004.

Mitasova, H., Mitas, L., and Harmon, R. S.: Simultaneous spline approximation and topographic analysis for lidar elevation data in open-source GIS, IEEE Geoscience and Remote Sensing Letters, 2, 375–379, https://doi.org/10.1109/LGRS.2005.848533, 2005.

Mitasova, H., Barton, M., Ullah, I., Hofierka, J., and Harmon, R.: 3.9 GIS-Based Soil Erosion Modeling, in: Treatise on Geomorphology, edited by Shroder, J. F., chap. 3.9, pp. 228–258, Elsevier, San Diego, California, USA, https://doi.org/10.1016/B978-0-12-374739-6.00052-X, http://www.sciencedirect.com/science/article/pii/B978012374739600052X, 2013.

Moore, I. and Burch, G.: Modeling Erosion and Deposition: Topographic Effects, Transactions of the American Society of Agricultural Engineers, 29, 1624–1640, 1986.

Renard, K. G., Foster, G. R., Weesies, G. A., McCool, D. K., and Yoder, D. C.: Predicting soil erosion by water: a guide to conservation planning with the Revised Universal Soil Loss Equation (RUSLE), Tech. Rep. 703, US Government Printing Office, Washington, DC, https://www.ars.usda.gov/ARSUserFiles/64080530/rusle/ah_703.pdf, 1997.

Shobe, C. M., Tucker, G. E., and Barnhart, K. R.: The SPACE 1.0 model: A Landlab component for 2-D calculation of sediment transport, bedrock erosion, and landscape evolution, Geoscientific Model Development, 10, 4577–4604, https://doi.org/10.5194/gmd-10-4577-2017, 2017.

Sorrie, B. A.: An Inventory of the Significant Natural Areas of Hoke County, North Carolina, Tech. rep., North Carolina Natural Heritage Program, 2004.

Sorrie, B. A., Gray, J. B., and Crutchfield, P. J.: The Vascular Flora of the Longleaf Pine Ecosystem of Fort Bragg and Weymouth Woods, North Carolina, Castanea, 71, 129–161, https://doi.org/10.2179/05-02.1, 2006.

Starek, M. J., Mitasova, H., Hardin, E., Weaver, K., Overton, M., and Harmon, R. S.: Modeling and analysis of landscape evolution using airborne , terrestrial , and laboratory laser scanning, Geosphere, 7, 1340–1356, https://doi.org/10.1130/GES00699.1, 2011.

Temme, A., Schoorl, J., Claessens, L., and Veldkamp, A.: 2.13 Quantitative Modeling of Landscape Evolution, vol. 2, Elsevier Ltd., https://doi.org/10.1016/B978-0-12-374739-6.00039-7, http://linkinghub.elsevier.com/retrieve/pii/B9780123747396000397, 2013.

Thaxton, C. S.: Investigations of grain size dependent sediment transport phenomena on multiple scales, Phd, North Carolina State University, http://www.lib.ncsu.edu/resolver/1840.16/3339, 2004.

Thomas, J. T., Iverson, N. R., Burkart, M. R., and Kramer, L. A.: Long-term growth of a valley-bottom gully, Western Iowa, Earth Surface Processes and Landforms, 29, 995–1009, https://doi.org/10.1002/esp.1084, 2004.

Tucker, G., Lancaster, S., Gasparini, N., and Bras, R.: The channel-hillslope integrated landscape development model (CHILD), in: Landscape erosion and evolution modeling, pp. 349–388, Springer, Boston, MA, https://doi.org/10.1007/978-1-4615-0575-4_12, 2001.

Webb, R. and Wilshire, H.: Environmental Effects of Off-Road Vehicles: Impacts and Management in Arid Regions, Environmental Management Series, Springer New York, https://doi.org/10.1007/978-1-4612-5454-6, 1983.

Willgoose, G.: Mathematical Modeling of Whole Landscape Evolution, Annual Review of Earth and Planetary Sciences, 33, 443–459, https://doi.org/10.1146/annurev.earth.33.092203.122610, http://www.annualreviews.org/doi/10.1146/annurev.earth.33.092203.122610, 2005.

Wischmeier, W. H., Smith, D. D., Science, U. S., Administration, E., and Station, P. U. A. E.: Predicting Rainfall Erosion Losses: A Guide to Conservation Planning, Tech. rep., Washington, D.C., https://naldc.nal.usda.gov/download/CAT79706928/, 1978.

Yin, S., A. Nearing, M., Borrelli, P., and Xue, X.: Rainfall Erosivity: An Overview of Methodologies and Applications, Vadose Zone Journal, 16, https://doi.org/10.2136/vzj2017.06.0131, 2017.

Zahra, T., Paudel, U., Hayakawa, Y., and Oguchi, T.: Knickzone Extraction Tool (KET) – A New ArcGIS toolset for automatic extraction of knickzones from a DEM based on multi-scale stream gradients, Open Geosciences, 9, https://doi.org/10.1515/geo-2017-0006, 2017.